EMORY LIBRARIES & INFORMATION TECHNOLOGY

OpenEmory

Differential Impairment of Thalamocortical Structural Connectivity in Amyotrophic Lateral Sclerosis

Jiu-Quan Zhang, *Third Military Medical University*
Bing Ji, *Emory University*
Chao-Yang Zhou, *Third Military Medical University*
Longchuan Li, *Emory University*
Zhihao Li, *Emory University*
Xiaoping Hu, *Emory University*
Jun Hu, *Third Military Medical University*

Journal Title: CNS Neuroscience and Therapeutics
Volume: Volume 23, Number 2
Publisher: Wiley Open Access | 2017-02-01, Pages 155-161
Type of Work: Article | Final Publisher PDF
Publisher DOI: 10.1111/cns.12658
Permanent URL: https://pid.emory.edu/ark:/25593/ts4fm

Final published version: http://dx.doi.org/10.1111/cns.12658

Copyright information:

© 2016 John Wiley & Sons Ltd
This is an Open Access work distributed under the terms of the Creative Commons Attribution 4.0 International License (https://creativecommons.org/licenses/by/4.0/).

Accessed December 8, 2019 11:02 AM EST

CNS Neuroscience & Therapeutics

ORIGINAL ARTICLE

CNS Neuroscience & Therapeutics

Differential Impairment of Thalamocortical Structural Connectivity in Amyotrophic Lateral Sclerosis

Jiu-Quan Zhang,[1,2] Bing Ji,[2] Chao-Yang Zhou,[1] Long-Chuan Li,[2,3] Zhi-Hao Li,[2,4] Xiao-Ping Hu[5] & Jun Hu[6]

1 Department of Radiology, Southwest Hospital, Third Military Medical University, Chongqing, China
2 Biomedical Imaging Technology Center, Emory University/Georgia Institute of Technology, Atlanta, GA, USA
3 Marcus Autism Center, Children's Healthcare of Atlanta, Emory University, Atlanta, GA, USA
4 Institute of affective and Social Neuroscience, Shenzhen University, Shenzhen, Guangdong, China
5 Department of Bioengineering, University of California, Riverside, CA, USA
6 Department of Neurology, Southwest Hospital, Third Military Medical University, Chongqing, China

Keywords
Amyotrophic lateral sclerosis; Diffusion tensor imaging; Probabilistic tractography; Thalamocortical connectivity.

Correspondence
X. Hu, Department of Bioengineering, University of California, Riverside, CA 92521, USA.
Tel.: +1-951-827-2925;
Fax: +1-951-827-6416;
E-mail: xhu@engr.ucr.edu
or
J. Hu, Department of Neurology, Southwest Hospital, Third Military Medical University, Chongqing 400038, China.
Tel.: +86-23-6875-4419;
Fax: +86-23-6546-3725;
E-mail: hujun_1978@163.com
Received 23 July 2016; revision 8 October 2016; accepted 9 October 2016

SUMMARY

Aims: The thalamus is a major relay station that modulates input from many cortical areas and a filter for sensory input and is involved in the pathophysiology of amyotrophic lateral sclerosis (ALS). However, it still remains unclear whether all thalamocortical networks are affected or whether there is selective vulnerability. In this study, we aimed to study the selective vulnerability of different thalamocortical structural connections in ALS and to test the hypothesis of a specific impairment in motor-related thalamocortical connectivity. **Methods:** Diffusion tensor imaging (DTI) tractography was used to identify thalamocortical structural pathways in 38 individuals with ALS and 35 gender/age-matched control subjects. Thalami of both groups were parcellated into subregions based on local patterns of thalamocortical connectivity. DTI measures of these distinct thalamocortical connections were derived and compared between groups. **Results:** The analysis of probabilistic tractography showed that the structural connectivity between bilateral pre/primary motor cortices and associated thalamic subregions was specifically impaired in patients with ALS, while the other thalamocortical connections remained relatively intact. In addition, fractional anisotropy values of the impaired thalamocortical motor pathway were inversely correlated with the disease duration. **Conclusion:** Our findings provide direct evidence for selective impairment of the thalamocortical structural connectivity in ALS.

doi: 10.1111/cns.12658

The first two authors contributed equally to this work.

Introduction

Amyotrophic lateral sclerosis (ALS) is a neurodegenerative disease characterized by progressive upper and lower motor neuron degeneration [1]. Although motor cortex impairment is the hallmark feature of ALS, there is increasing evidence indicating the involvement of widespread extramotor brain areas [2–5]. Particularly, as a major relay station in the brain that modulates input from many cortical areas and a filter for sensory input [6], the involvement of the thalamus in ALS has been reported by a number of studies using diffusion MRI [7,8], MR spectroscopy [9], fMRI [10], CT perfusion [11], and PET [12,13].

The thalamus and cerebral cortex are connected via topographically organized white matter tracks with parallel pathways, linking distinct cortical areas to specific thalamic nuclei [14,15]. However, while numerous studies have reported thalamic abnormalities in ALS, it still remains unclear whether all thalamocortical networks are affected equally in ALS, or whether there is selective impairment.

Until recently, *in vivo* examination of individual thalamocortical networks has been challenging. Conventional fMRI requires multiple fine-tuned cognitive paradigms to reliably activate distinct cortical areas and their associated thalamic counterparts [16]. Fortunately, recent development of connectivity analysis with

© 2016 John Wiley & Sons Ltd

diffusion tensor imaging (DTI) has enabled us to approach this challenge with probabilistic tractography and connectivity-based segmentation [17–19]. In this analysis, it is possible to separate regions of differing specialization of the human cortex by utilizing underlying white matter pathways [20].

In this work, we used tractography-based thalamus parcellation to identify different thalamic subregions [19,21] and to further elucidate possible differentially affected thalamocortical networks in ALS. Based on existing knowledge about ALS, we hypothesized that motor-related thalamocortical connectivity would be affected in ALS.

Materials and Methods

Participants

Thirty-eight individuals (25 males/13 females) with a diagnosis of sporadic probable, or definite ALS, according to the revised El Escorial criteria [22], were recruited from the Department of Neurology at Southwest Hospital in Chongqing, China. Clinical status of the participants was assessed by the ALS Functional Rating Scale-Revised (ALSFRS-R) [23] within 12 h after the MRI scan. Disease duration was calculated from symptom onset to the scan date in months, and the rate of disease progression was defined as follows: (48 − ALSFRS-R score)/(disease duration) [24–26]. None of the patients included in this study received any specific treatment. Exclusion criteria were as follows: (1) family history of motor neuron diseases, (2) clinical diagnosis of frontotemporal dementia [27], (3) the presence of other major systemic, psychiatric, or neurological illnesses, and (4) cognitive impairment (score < 26), as determined by the Montreal Cognitive Assessment [28].

Thirty-five healthy controls (21 males/14 females) with no previous history of neurological or psychiatric diseases and with normal brain MRI scans were recruited from the local community. All the participants were right-handed according to the Edinburgh Inventory [29].

This study was approved by the Medical Research Ethics Committee of Southwest Hospital, and written informed consent was obtained from all the participants.

Data Acquisition

MRI data were obtained from a 3T scanner of Siemens Tim Trio (Siemens, Erlangen, Germany) with an eight-channel head coil. The DTI data were acquired in two identical scans using a single-shot twice refocused spin-echo diffusion echo-planar imaging sequence with the following parameters: repetition time (TR) = 10,000 ms, echo time (TE) = 92 ms, 64 diffusion directions with b = 1000 s/mm^2 and an additional volume with b = 0 s/mm^2, matrix = 128 × 124, field of view = 256 × 248 mm^2, 75 axial slices with 2 mm in thickness and without gap. High-resolution sagittal structural images were acquired using a 3D magnetization-prepared rapid gradient echo sequence using the following parameters: TR = 1900 ms, TE = 2.52 ms, inversion time = 900 ms, flip angle (FA) = 9°, matrix = 256 × 256, thickness = 1.0 mm, no gap, voxel size = 1 × 1 × 1 mm^3.

The present DTI analysis of structural connectivity involved probabilistic fiber tracking through different subregions of the thalamus. For this purpose, an independent sample was needed for an unbiased parcellation of the thalamus. This independent sample was obtained from the Human Connectome Project (HCP; www.humanconnectomeproject.org), an open-access repository of healthy human brain datasets [30]. Subjects of HCP were scanned with a customized 3T Siemens scanner (Connectome Skyra) using a single-shot, single refocusing spin-echo, echo-planar imaging sequence. Eighty subjects (32 males/48 females; aged: 22–36 years) from the HCP dataset of "WU-Minn" (The Washington University and University of Minnesota) were used in this study. The detailed imaging protocol could be found at https://www.humanconnectome.org/documentation/Q1/imaging-protocols.html.

Data Preprocessing

Our DTI data were preprocessed using the FMRIB's Diffusion Toolbox included in the FMRIB's Software Library (FSL, http://www.fmrib.ox.ac.uk/fsl) [31,32]. The preprocessing steps for DTI data included correction of eddy current distortion, brain extraction, diffusion tensor fitting, and estimation of diffusion orientation distribution functions. DTI data of the independent HCP sample were obtained and preprocessed using HCP's diffusion preprocessing pipeline [33,34].

Masks of Thalamus and Cerebral Cortex

The DTI-based fiber tracking involved 3D masks in both thalamus and cerebral cortex. The mask of the thalamus was extracted from the Harvard-Oxford subcortical structural atlas in the MNI space (http://fsl.fmrib.ox.ac.uk/fsl/fslwiki/Atlases) and voxels located in ventricles or white matter regions were removed (Figure 1A). In the cortex, seven masks were adopted from a previous study [19,35] in each hemisphere including bilateral (1) prefrontal cortex (PFC), (2) premotor cortex (PMC), (3) primary motor cortex (M1), (4) somatosensory cortex (SC), (5) parietal cortex (PC), (6) occipital cortex (OC), and (7) temporal cortex (TC).

Thalamus Parcellation Based on HCP Data

Probabilistic tractography was used to delineate white matter pathways from the thalamus to the cerebral cortex. The algorithm accommodated crossing fibers in each voxel [21] by sending 5000 tracks from each voxel in the thalamus to the seven ipsilateral cortical regions. As a result, a probabilistic map of connections for each of the seven cortical targets was generated. Then, thalamus voxels of each participant were classified based on their strongest cortical connectivity (winner-take-all) into seven subregions [19]. After transforming individual parcellations into the MNI space, the algorithm of "Simultaneous Truth and Performance Level" (STAPLE) was applied to fuse individual segmentations [36]. The STAPLE approach was used to combine manual tracings of the same subject from multiple raters and to estimate the hidden "ground truth" consensus from a probabilistic model.

After fusing segmentation results across individuals in the HCP sample, the merged result (Figure 1B) was transformed from the MNI space back into the individual diffusion space for subsequent analyses of different thalamocortical connections.

 © 2016 John Wiley & Sons Ltd

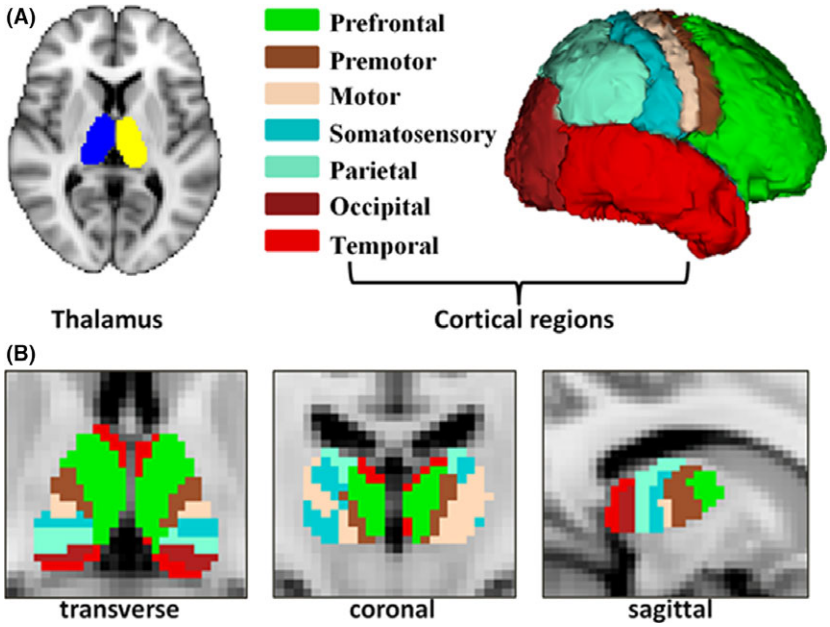

Figure 1 (**A**) Seed and target region-of-interests used for tractography. Thalami were generated from each participant's T1 image. Targets for tractography were the prefrontal, premotor, motor, somatosensory, parietal, occipital, and temporal cortices. (**B**) Structural connectivity-based parcellated thalami and their subregions obtained using tractography in transverse, coronal, and sagittal view.

Thalamocortical Tractography in the Recruited Sample

Here, probabilistic tractography was performed between each thalamic subregion and its ipsilateral counterpart in the cortex. The thalamus and cortex regions mutually served as seed and target in two symmetric tractography ran so that the direction effect was removed. After 5000 samples sent from each seed voxel, the maps of streamline counts between each seed and target pair were normalized by the total number of samples (5000) multiplied with the voxel number in the seed mask and thresholded at 5, 10, and 25% [18]. These thresholded and binarized masks were further evaluated on across-subject reproducibility, and the most reproducible one was subsequently utilized as tract-based region-of-interests from which DTI measures (FA, axial diffusivity (AD, diffusion parallel to the axon fibers), radial diffusivity (RD, diffusivity perpendicular to the axonal fibers, and mean diffusivity (MD, a mean of all three eigenvalues of the diffusion tensor) were extracted for group comparison.

Reproducibility of Thresholded Track Pathways

The reproducibility of thresholded track pathways was defined by spatial overlap across individuals and quantified by the Overlap By Pairs (OBP) [37]. If a group includes m pairs of images, with m representing different subjects and A/B corresponding to the mask, the following formula can be obtained:

$$\mathrm{OBP} = \frac{\sum_m (\mathrm{A_m} \cap \mathrm{B_m})}{\sum_m (\mathrm{A_m} \cup \mathrm{B_m})}$$

DTI Measures

DTI measures of FA, MD, AD, and RD were extracted from the 5% binarized (most reproducible, see results below) probability maps of structural connectivity. All DTI measures were compared between groups with independent (two) sample *t*-tests using MATLAB Release 2012b (The MathWorks, Inc., Natick, MA, USA).

Results

Demographic and Clinical Data

The demographic and clinical characteristics of the present sample are summarized in Table 1. All individuals with ALS exhibited clinical signs of upper and lower motor neuron involvement. Seven individuals with ALS were classified as "bulbar onset," thirty as "limb onset," and one as "both bulbar and limb onsets." Independent sample *t*-test for age and two samples Kolmogorov–

Table 1 Demographic data of the participants

	Patient	Control	*P* value
Age (years)	48.5 ± 9.37	48.8 ± 11.3	0.89
Male:female	25/13	21/14	0.73
El Escorial criteria (probable/definite)	24/14	–	–
Limb/bulbar/both onset	30/7/1	–	–
Disease duration (months)	21.3 ± 18.0	–	–
ALSFRS-R	31.2 ± 6.57	–	–
Disease progression rate	1.35 ± 1.26	–	–

© 2016 John Wiley & Sons Ltd

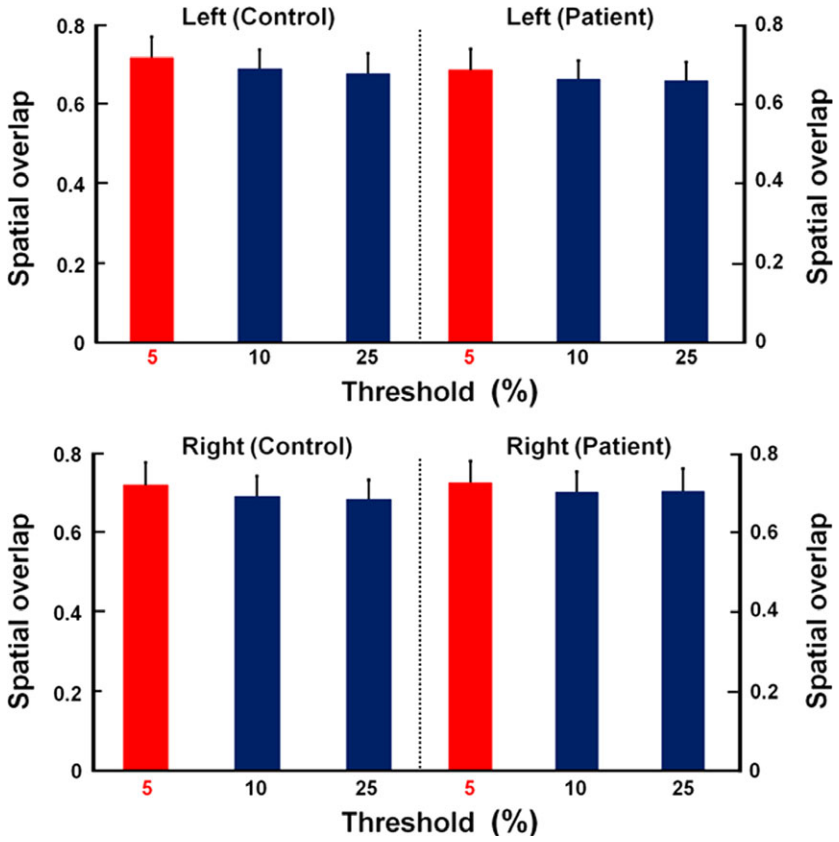

Figure 2 Spatial overlap rates of bilateral thalamocortical structural connectivity from each thalamic subregion to its corresponding cortex in patients and controls at the probabilistic thresholds of 5, 10, and 25%. Spatial overlap was highest at a threshold of 5%.

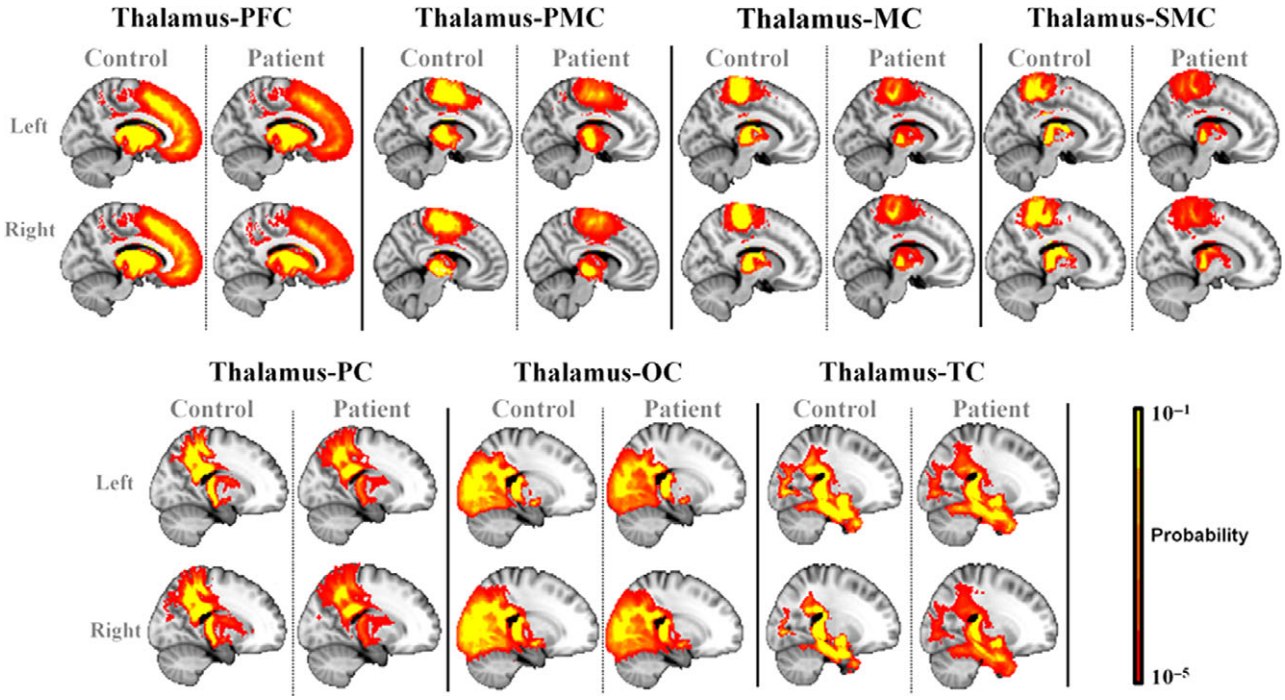

Figure 3 Probabilistic tractography maps between left/right thalamic subregions and ipsilateral specific cortex regions were presented at a threshold of 5% in patients with ALS and healthy controls.

 © 2016 John Wiley & Sons Ltd

Table 2 Statistical analysis for 5% connection results (FA, MD, AD, RD)

		FA		MD ($\times 10^{-4}$ mm^2/s)		AD ($\times 10^{-3}$ cm^2/s)		RD ($\times 10^{-4}$ cm^2/s)	
Connection	Group	Mean	SD	Mean	SD	Mean	SD	Mean	SD
L-Thalamus-PFC	Control	0.320	0.0142	9.60	0.560	1.25	0.058	8.16	0.564
	Patient	0.314	0.0165	9.63	0.700	1.25	0.072	8.23	0.699
L-Thalamus-PMC	Control	**0.376**	**0.0155**	9.08	0.414	1.25	0.044	7.38	0.426
	Patient	**0.364**[a]	**0.0178**	9.19	0.609	1.25	0.063	7.54	0.594
L-Thalamus-M1	Control	**0.371**	**0.0152**	9.11	0.440	1.25	0.046	7.44	0.448
	Patient	**0.362**[b]	**0.0194**	9.17	0.642	1.25	0.071	7.54	0.623
L-Thalamus-SC	Control	0.350	0.0160	9.33	0.519	1.25	0.055	7.75	0.524
	Patient	0.347	0.0181	9.31	0.688	1.25	0.078	7.73	0.660
L-Thalamus-PC	Control	0.342	0.0161	9.23	0.532	1.24	0.056	7.67	0.536
	Patient	0.341	0.0166	9.20	0.653	1.23	0.072	7.64	0.630
L-Thalamus-OC	Control	0.324	0.0153	9.05	0.429	1.20	0.044	7.57	0.439
	Patient	0.323	0.0172	9.16	0.619	1.21	0.064	7.68	0.619
L-Thalamus-TC	Control	0.311	0.0164	9.45	0.501	1.23	0.048	8.04	0.521
	Patient	0.306	0.0180	9.52	0.630	1.23	0.064	8.13	0.635
R-Thalamus-PFC	Control	0.319	0.0158	9.56	0.580	1.24	0.055	8.13	0.602
	Patient	0.313	0.0164	9.63	0.700	1.25	0.067	8.24	0.638
R-Thalamus-PMC	Control	**0.375**	**0.0153**	9.02	0.410	1.24	0.042	7.34	0.428
	Patient	**0.365**[c]	**0.0190**	9.17	0.630	1.25	0.068	7.52	0.621
R-Thalamus-M1	Control	**0.371**	**0.0144**	9.04	0.421	1.24	0.045	7.38	0.429
	Patient	**0.362**[d]	**0.0174**	9.13	0.651	1.24	0.071	7.50	0.634
R-Thalamus-SC	Control	0.346	0.0157	9.32	0.483	1.25	0.505	7.76	0.489
	Patient	0.343	0.0183	9.31	0.719	1.24	0.080	7.76	0.691
R-Thalamus-PC	Control	0.341	0.0137	9.20	0.457	1.23	0.050	7.65	0.450
	Patient	0.340	0.0182	9.18	0.631	1.23	0.071	7.63	0.606
R-Thalamus-OC	Control	0.326	0.0119	9.02	0.339	1.20	0.039	7.53	0.327
	Patient	0.322	0.0161	9.15	0.602	1.21	0.062	7.68	0.601
R-Thalamus-TC	Control	0.311	0.0132	9.30	0.429	1.21	0.045	7.89	0.432
	Patient	0.304	0.0174	9.41	0.565	1.22	0.052	8.04	0.574

The bold values indicate that there are statistical differences between groups.
[a]$t = 3.05$, $P = 0.003$. [b]$t = 2.34$, $P = 0.02$. [c]$t = 2.52$, $P = 0.01$. [d]$t = 2.24$, $P = 0.03$.

Smirnov test for gender were performed and showed nonsignificant group difference on both variables.

Group Differences in Thalamocortical Connectivity

Connectivity-based thalamus parcellation in the HCP sample is shown in Figure 1B.

In Figure 2, measures of spatial overlap for binarized probability maps are compared at thresholds of 5, 10, and 25%. The across-subject overlap was highest at the threshold of 5%.

In Figure 3, probabilistic tractography maps are compared between groups at the threshold of 5% for the seven thalamocortical pathways.

Group comparisons of DTI measures (FA, MD, AD, and RD) of the seven thalamocortical connections at a threshold of 5% are detailed in Table 2 (the results at thresholds of 10 and 25% are shown in the Tables S1 and S2, respectively). At the threshold of 5%, FA values of the bilateral premotor (left thalamus-PMC, $t = 3.05$, $P = 0.003$; right thalamus-PMC, $t = 2.52$, $P = 0.01$) and motor (left thalamus-M1, $t = 2.34$, $P = 0.02$; right thalamus-M1, $t = 2.24$, $P = 0.03$) pathways were significantly decreased in the ALS group.

Imaging and Clinical Measures Correlation Analyses

To investigate potential correlations between the imaging metrics and clinical variables, Pearson's correlations were calculated. As shown in Figure 4, significant negative correlations were noted between the FA of bilateral thalamocortical connections in premotor (left: $P = 0.002$; right: $P = 0.03$; Figure 4A) and motor (left: $P = 0.004$; right: $P < 0.001$; Figure 4B) pathways. There were no other significant associations between imaging findings and clinical data.

Discussion

In vivo neuroimaging [8,9,12,38] and postmortem neuropathological studies [3,39,40] have both confirmed thalamic involvement in ALS. Extending from these previous studies, the present study capitalized on tractography-based thalamus parcellation and probabilistic tractography to examine differential impairment of thalamocortical structural connectivity. We found that the structural connectivity of thalamocortical pathways associated with PMC and M1 was both impaired in ALS, while the other thalamocortical connections remained relatively intact. In addition, FA values

© 2016 John Wiley & Sons Ltd

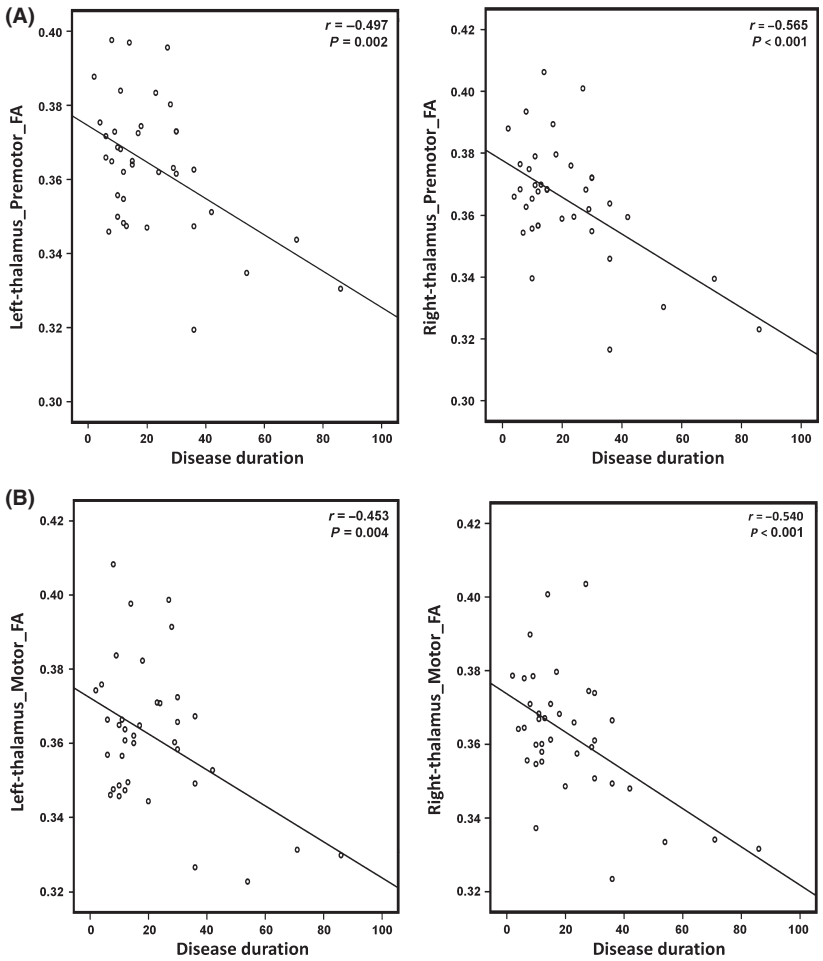

Figure 4 (**A**) Correlation analyses revealed a significant inverse correlation between the FA of the tract connecting the thalamus and bilateral motor cortices (left, r = −0.453, *P* = 0.004; right, r = −0.540, *P* < 0.001) and the disease duration. (**B**) Correlation analyses revealed a significant inverse correlation between the FA of the tract connecting the thalamus and bilateral M1 cortices (left, r = −0.453, *P* = 0.004; right, r = −0.540, *P* < 0.001) and the disease duration.

of the impaired thalamocortical structural connectivity were inversely correlated with the disease duration.

Differential Vulnerability of Thalamocortical Structural Connectivity

The present data suggest that the thalamocortical motor connectivity is prominently affected in ALS. Given the apparent motor disabilities in individuals with ALS, these findings are perhaps not surprising. However, previous neuroimaging studies have not directly examined potential selective impairment in different thalamocortical connections. Our results indicate that structural networks linking the cortex to the thalamus are differentially affected in ALS. This finding is consistent with the four-stage neuropathological model proposed by Braak et al. [41,42], which suggests that the involvement of the thalamus sequentially starts in the ventrolateral posterior thalamic nucleus, progresses to the ventral anterior thalamic nucleus and the mediodorsal thalamic nucleus, and eventually covers the whole thalamus. Correspondingly, cortical impairments progress from the primary motor cortex to the premotor cortex.

Relationship of Neuroimaging and Clinical Measures

We revealed strong inverse correlations between ALS duration and FA decrement in motor-related thalamocortical pathways. These findings may be valuable for assessing the progression of ALS and could be considered as an *in vivo* imaging biomarker [43]. They also suggest that further studies using more specific motor function evaluation may be helpful in screening whether motor dysfunction is related to distinct patterns of thalamocortical structural connectivity alterations.

Limitation

The main limitation of the current study is the lack of a detailed evaluation of the motor status in individuals with ALS, which prevented

 © 2016 John Wiley & Sons Ltd

us from examining the association between imaging measures and clinical symptoms, weakening the interpretation of our results.

Acknowledgments

This work was supported by funds from the National Natural Science Foundation of China (Grant No. 81200882, 31671169), the Natural Science Foundation of Chongqing (Grant No. CSTC2016jcyjA2163), and the Natural Science Foundation of SZU (Grant No. 201564, 000099).

Conflict of Interest

The authors declare no conflict of interest.

References

1. Kiernan MC, Vucic S, Cheah BC, et al. Amyotrophic lateral sclerosis. *Lancet* 2011;**377**:942–955.
2. Pradat PF, Bruneteau G, Munerati E, et al. Extrapyramidal stiffness in patients with amyotrophic lateral sclerosis. *Mov Disord* 2009;**24**:2143–2148.
3. Desai J, Swash M. Extrapyramidal involvement in amyotrophic lateral sclerosis: Backward falls and retropulsion. *J Neurol Neurosurg Psychiatry* 1999;**67**:214–216.
4. Verstraete E, Veldink JH, van den Berg LH, van den Heuvel MP. Structural brain network imaging shows expanding disconnection of the motor system in amyotrophic lateral sclerosis. *Hum Brain Mapp* 2014;**35**:1351–1361.
5. Agosta F, Pagani E, Rocca MA, et al. Voxel-based morphometry study of brain volumetry and diffusivity in amyotrophic lateral sclerosis patients with mild disability. *Hum Brain Mapp* 2007;**28**:1430–1438.
6. Sherman S, Guillery R. *Exploring the Thalamus and Its Role in Cortical Function*, 2nd edn. Cambridge, MA: MIT Press, 2006.
7. Thivard L, Pradat PF, Lehericy S, et al. Diffusion tensor imaging and voxel based morphometry study in amyotrophic lateral sclerosis: Relationships with motor disability. *J Neurol Neurosurg Psychiatry* 2007;**78**:889–892.
8. Sharma KR, Sheriff S, Maudsley A, Govind V. Diffusion tensor imaging of basal ganglia and thalamus in amyotrophic lateral sclerosis. *J Neuroimaging* 2013;**23**:368–374.
9. Sharma KR, Saigal G, Maudsley AA, Govind V. 1H MRS of basal ganglia and thalamus in amyotrophic lateral sclerosis. *NMR Biomed* 2011;**24**:1270–1276.
10. Lule D, Diekmann V, Muller HP, Kassubek J, Ludolph AC, Birbaumer N. Neuroimaging of multimodal sensory stimulation in amyotrophic lateral sclerosis. *J Neurol Neurosurg Psychiatry* 2010;**81**:899–906.
11. Murphy MJ, Grace GM, Tartaglia MC, et al. Widespread cerebral haemodynamics disturbances occur early in amyotrophic lateral sclerosis. *Amyotroph Lateral Scler* 2012;**13**:202–209.
12. Turner MR, Cagnin A, Turkheimer FE, et al. Evidence of widespread cerebral microglial activation in amyotrophic lateral sclerosis: An [11C](R)-PK11195 positron emission tomography study. *Neurobiol Dis* 2004;**15**:601–609.
13. Abrahams S, Goldstein LH, Kew JJ, et al. Frontal lobe dysfunction in amyotrophic lateral sclerosis. A PET study. *Brain* 1996;**119**(Pt 6):2105–2120.
14. Alexander GE, DeLong MR, Strick PL. Parallel organization of functionally segregated circuits linking basal ganglia and cortex. *Annu Rev Neurosci* 1986;**9**:357–381.
15. Haber SN. The primate basal ganglia: Parallel and integrative networks. *J Chem Neuroanat* 2003;**26**:317–330.
16. Woodward ND, Karbasforoushan H, Heckers S. Thalamocortical dysconnectivity in schizophrenia. *Am J Psychiatry* 2012;**169**:1092–1099.
17. Nair A, Treiber JM, Shukla DK, Shih P, Müller R-A. Impaired thalamocortical connectivity in autism spectrum disorder: A study of functional and anatomical connectivity. *Brain* 2013;**136**:1942.
18. Bohanna I, Georgiou-Karistianis N, Egan GF. Connectivity-based segmentation of the striatum in Huntington's disease: Vulnerability of motor pathways. *Neurobiol Dis* 2011;**42**:475–481.
19. Behrens TE, Johansen-Berg H, Woolrich MW, et al. Non-invasive mapping of connections between human thalamus and cortex using diffusion imaging. *Nat Neurosci* 2003;**6**:750–757.
20. Klein JC, Behrens TE, Robson MD, Mackay CE, Higham DJ, Johansen-Berg H. Connectivity-based parcellation of human cortex using diffusion MRI: Establishing reproducibility, validity and observer independence in BA 44/45 and SMA/pre-SMA. *NeuroImage* 2007;**34**:204–211.
21. Behrens TE, Berg HJ, Jbabdi S, Rushworth MF, Woolrich MW. Probabilistic diffusion tractography with multiple fibre orientations: What can we gain? *NeuroImage* 2007;**34**:144–155.
22. Brooks BR, Miller RG, Swash M, Munsat TL. World Federation of Neurology Research Group on Motor Neuron D. El Escorial revisited: Revised criteria for the diagnosis of amyotrophic lateral sclerosis. *Amyotroph Lateral Scler Other Motor Neuron Disord* 2000;**1**:293–299.
23. Cedarbaum JM, Stambler N, Malta E, et al. The ALSFRS-R: A revised ALS functional rating scale that incorporates assessments of respiratory function. BDNF ALS Study Group (Phase III). *J Neurol Sci* 1999;**169**:13–21.
24. Bastin ME, Pettit LD, Bak TH, Gillingwater TH, Smith C, Abrahams S. Quantitative tractography and tract shape modeling in amyotrophic lateral sclerosis. *J Magn Reson Imaging* 2013;**38**:1140–1145.
25. van der Graaff MM, Sage CA, Caan MW, et al. Upper and extra-motoneuron involvement in early motoneuron disease: A diffusion tensor imaging study. *Brain* 2011;**134**:1211–1228.
26. Verstraete E, Veldink JH, Hendrikse J, Schelhaas HJ, van den Heuvel MP, van den Berg LH. Structural MRI reveals cortical thinning in amyotrophic lateral sclerosis. *J Neurol Neurosurg Psychiatry* 2012;**83**:383–388.
27. Neary D, Snowden JS, Gustafson L, et al. Frontotemporal lobar degeneration: A consensus on clinical diagnostic criteria. *Neurology* 1998;**51**:1546–1554.
28. Nasreddine ZS, Phillips NA, Bedirian V, et al. The Montreal Cognitive Assessment, MoCA: A brief screening tool for mild cognitive impairment. *J Am Geriatr Soc* 2005;**53**:695–699.
29. Oldfield RC. The assessment and analysis of handedness: The Edinburgh inventory. *Neuropsychologia* 1971;**9**:97–113.
30. Van Essen DC, Ugurbil K, Auerbach E, et al. The Human Connectome Project: A data acquisition perspective. *NeuroImage* 2012;**62**:2222–2231.
31. Smith SM, Jenkinson M, Woolrich MW, et al. Advances in functional and structural MR image analysis and implementation as FSL. *NeuroImage* 2004;**23**:S208–S219.
32. Woolrich MW, Jbabdi S, Patenaude B, et al. Bayesian analysis of neuroimaging data in FSL. *NeuroImage* 2009;**45**:S173–S186.
33. Glasser MF, Sotiropoulos SN, Wilson JA, et al. The minimal preprocessing pipelines for the Human Connectome Project. *NeuroImage* 2013;**80**:105–124.
34. Sotiropoulos SN, Jbabdi S, Xu J, et al. Advances in diffusion MRI acquisition and processing in the Human Connectome Project. *NeuroImage* 2013;**80**:125–143.
35. Ji B, Li Z, Li K, et al. Dynamic thalamus parcellation from resting-state fMRI data. *Hum Brain Mapp* 2016;**37**:954–967.
36. Warfield SK, Zou KH, Wells WM. Simultaneous truth and performance level estimation (STAPLE): An algorithm for the validation of image segmentation. *IEEE Trans Med Imaging* 2004;**23**:903–921.
37. Crum WR, Camara O, Hill DL. Generalized overlap measures for evaluation and validation in medical image analysis. *IEEE Trans Med Imaging* 2006;**25**:1451–1461.
38. Sach M, Winkler G, Glauche V, et al. Diffusion tensor MRI of early upper motor neuron involvement in amyotrophic lateral sclerosis. *Brain* 2004;**127**:340–350.
39. Takeda T, Uchihara T, Chikugo T, Hiraga T, Kitaguchi M, Kojima H. Preferential involvement of the basolateral limbic circuit in an amyotrophic lateral sclerosis patient. *Eur J Neurol* 2007;**14**:e5–e6.
40. Seilhean D, Takahashi J, El Hachimi KH, et al. Amyotrophic lateral sclerosis with neuronal intranuclear protein inclusions. *Acta Neuropathol* 2004;**108**:81–87.
41. Braak H, Brettschneider J, Ludolph AC, Lee VM, Trojanowski JQ, Del Tredici K. Amyotrophic lateral sclerosis–a model of corticofugal axonal spread. *Nat Rev Neurol* 2013;**9**:708–714.
42. Brettschneider J, Del Tredici K, Toledo JB, et al. Stages of pTDP-43 pathology in amyotrophic lateral sclerosis. *Ann Neurol* 2013;**74**:20–38.
43. Turner MR, Kiernan MC, Leigh PN, Talbot K. Biomarkers in amyotrophic lateral sclerosis. *Lancet Neurol* 2009;**8**:94–109.

Supporting Information

The following supplementary material is available for this article:

Table S1. Statistical analysis for 10% connection results (FA, MD, AD, RD).

Table S2. Statistical analysis for 25% connection results (FA, MD, AD, RD).

© 2016 John Wiley & Sons Ltd